

# INVERSE SCATTERING TRANSFORMS FOR THE SIXTH-ORDER NONLINEAR SCHRÖDINGER EQUATION WITH ZERO/NONZERO BOUNDARY CONDITIONS: BOUND-STATE SOLITON AND ROGUE WAVE

WEIQI PENG AND YONG CHEN\*

ABSTRACT. In this work, inverse scattering transforms for the sixth-order nonlinear Schrödinger equation with zero/nonzero boundary conditions is given. Based on our analysis, the bound-state soliton and rogue wave solutions are obtained respectively. In terms of the Laurent's series and generalization of the residue theorem, the bound-state soliton is derived at zero boundary conditions. Using the robust inverse scattering transform, we present a matrix Riemann-Hilbert problem of the sixth-order nonlinear Schrödinger equation with nonzero boundary conditions. Then based on the obtained Riemann-Hilbert problem, the higher-order rogue wave solutions are derived through a modified Darboux transformation. Additionally, according to some appropriate parameters choices, several graphical analyses are provided to discuss the dynamical behaviors of the bound-state soliton and rogue wave solutions.

## 1. INTRODUCTION

The solutions of nonlinear evolution equations with zero boundary conditions (ZBCs) and nonzero boundary conditions (NZBCs) play a vital role in describing some relevant phenomena, and more and more researchers are interested in studying this topic. In the development of the past few decades, many techniques have been provided to find these solutions [1]- [4]. Of which, the inverse scattering transform (IST) method is the most powerful tool for analyzing initial value problems of integrable systems in soliton theory. The method was presented for the first time by Gardner et al. in 1967 for the KdV equation [5]. In a general way, the classical IST method was based on the Gel'fand-Levitan-Marchenko (GLM) integral equations. After that, Zakharov et al. properly simplified the IST method through developing a Riemann-Hilbert formulation [6]. Undergoes decades of development, the researches of Riemann-Hilbert formulation have made many successful progresses in the area of integrable systems, and it is still a hot topic today [7]- [17]. Especially, in recent years, using the Riemann-Hilbert method to research the bound-state soliton and rogue wave solutions has attracted many attentions.

The bound-state solitons, called multiple-poles soliton solutions, are generated when two or more fundamental solitons coexist with the same velocity and the same position. The multiple-poles soliton solutions for focusing nonlinear Schrödinger (NLS) equation was first derived by Zakharov and Shabat [18]. Since then, the multiple-poles solitons for various nonlinear integrable equations have been obtained, such as the sine-Gordon equation [19, 20], the modified KdV equation [21], the complex modified KdV equation [22], Wadati-Konno-Ichikawa equation [23], Sasa-Satsuma equation [25, 26]. As well as, asymptotic of multiple-pole solitons was analysed in [27, 28]. Generally, the IST method with GLM equation results in a complicated calculation for finding the bound-state solitons [20, 21], since some complicate limits need to be settled. However, through using the Laurent's series and generalization of the residue theorem [22-24], the Riemann-Hilbert problem (RHP) with multiple-poles can be solved directly, and the bound-state solitons can be expressed compactly.

Rogue waves have been constantly observed in various fields, which appear suddenly and disappear without trace, mainly possessing a high peak. In the study of the NLS equation, Peregrine first derived a kind of rational solution to describe rogue wave phenomena [29]. After that, the rogue waves have attracted the attention of more and more researchers. During this period, a lot of technologies have been developed to study the rogue waves, containing the Wronskian technique, the Darboux transformation (DT) method, the KP reduction method, etc. [30]- [35]. However, the standard IST is difficult to generate the rogue wave solution of the nonlinear integrable equations because of special regularity of the singular point. Until a wonderful and powerful approach, named robust inverse scattering transform, was pioneered by Bilman and Miller to research higher-order rogue wave solutions for the focusing NLS equation [36]. Suddenly, the robust inverse scattering transform has been employed to study the rogue waves for some nonlinear integrable model, including the Hirota equation [37], fifth-order nonlinear Schrödinger equation [38], generalized nonlinear Schrödinger equation [39], quartic nonlinear Schrödinger equation [40].

Nowadays, the investigation of high order NLS equations has attracted more and more attention, since they can describe many complex physical phenomena and possess more abundant dynamical behaviors than ones in the low order system. In this paper, we mainly focus on the sixth-order nonlinear Schrödinger (SONLS) equation [41]

$$iq_t + \frac{1}{2}q_{xx} + q|q|^2 + \delta K(q) = 0, \quad (1.1)$$

where

$$\begin{aligned}
K(q) = & q_{xxxxxx} + q^2 [60|q_x|^2 q^* + 50q_{xx}(q^*)^2 + 2q_{xxxx}^*] \\
& + q [12q^* q_{xxxx} + 18q_x^* q_{xxx} + 8q_x q_{xxx}^* + 70(q^*)^2 q_x^2 + 22|q_{xx}|^2] \\
& + 10q_x [3q^* q_{xxx} + 5q_x^* q_{xx} + 2q_x q_{xx}^*] + 10q^3 [2q^* q_{xx}^* + (q_x^*)^2] \\
& + 20q^* q_{xx}^2 + 20q|q|^6,
\end{aligned} \tag{1.2}$$

of which  $\delta$  is a arbitrary real constant.  $q(x, t)$  is a complex valued function with the real variables  $x$  and  $t$ . Eq.(1.1) can be applied to depict the propagation of pulses along optical fibers. In terms of the Hirota method, the soliton solutions of Eq.(1.1) were given in [42, 43]. The DT method is used to study the breather-to-soliton transition for the SONLS Eq.(1.1) in [44]. Recently, through the generalized DT method, the Modulation instability and rogue wave solutions for Eq.(1.1) were studied in [45]. Eq.(1.1) subjects to the following Lax pair [41]

$$\phi_x = U\phi = (ik\sigma_3 + Q)\phi, \quad \phi_t = V\phi = \sum_{m=0}^6 ik^m V_m \phi, \tag{1.3}$$

where

$$Q = \begin{pmatrix} 0 & iq^* \\ iq & 0 \end{pmatrix}, \quad \sigma_3 = \begin{pmatrix} 1 & 0 \\ 0 & -1 \end{pmatrix}, \quad V_m = \begin{pmatrix} A_m & B_m^* \\ B_m & -A_m \end{pmatrix}, \tag{1.4}$$

with

$$\begin{aligned}
A_0 = & -\frac{1}{2}|q|^2 - 10\delta|q|^6 - 5\delta [q^2 (q_x^*)^2 + (q^*)^2 q_x^2] - 10\delta|q|^2 (qq_{xx}^* + q^* q_{xx}) \\
& - \delta|q_{xx}|^2 + \delta(q_x q_{xxx}^* + q_x^* q_{xxx} - q^* q_{xxxx} - qq_{xxx}^*), \\
A_1 = & 12i\delta|q|^2 (q_x q^* - q_x^* q) + 2i\delta (q_x q_{xx}^* - q_x^* q_{xx} + q^* q_{xxx} - q_{xxx}^* q), \\
A_2 = & 1 + 12\delta|q|^4 - 4\delta|q_x|^2 + 4\delta (q_{xx}^* q + q_{xx} q^*), \quad A_3 = 8i\delta (qq_x^* - q^* q_x), \\
A_4 = & -16\delta|q|^2, \quad A_5 = 0, \quad A_6 = 32\delta, \quad B_2 = -24i\delta|q|^2 q_x - 4i\delta q_{xxx}, \quad B_4 = 16i\delta q_x, \\
B_0 = & \frac{i}{2} q_x + i\delta q_{xxxx} + 10i\delta (qq_x^* q_{xx} + qq_{xx}^* q_x + |q|^2 q_{xxx} + 3|q|^4 q_x + q_x |q_x|^2 + 2q^* q_x q_{xx}), \\
B_1 = & q + 12\delta q^* q_x^2 + 16\delta|q|^2 q_{xx} + 4\delta q^2 q_{xx}^* + 2\delta q_{xxxx} + 12\delta|q|^4 q + 8\delta q|q_x|^2, \\
B_3 = & -16\delta|q|^2 q - 8\delta q_{xx}, \quad B_5 = 32\delta q, \quad B_6 = 0,
\end{aligned} \tag{1.5}$$

where  $k$  is the spectrum parameter, the superscript  $*$  means the complex conjugate, and the function  $\phi$  is a  $2 \times 2$  eigenfunction matrix.

To the best knowledge of the authors, much research work has been done for the SONLS Eq.(1.1). However, the the bound-state soliton and rogue wave solutions for the SONLS Eq.(1.1) have never been analysed up to now. Therefore, the primary purpose of the present paper is to discuss the bound-state soliton and rogue wave solutions for the SONLS equation with zero/nonzero boundary conditions through Riemann-Hilbert method.

The outline of this paper is organized as follows: In section 2, we construct the reflection-less RHP with one higher-order poles, and obtain the multiple bound-state soliton solutions for the SONLS equation with zero boundary conditions. In section 3, we establish the RHP for the SONLS equation with nonzero boundary conditions using the robust inverse scattering transform. Then the RHP can be solved by a modified Darboux transformation, and the exact breather wave and rogue wave solutions are further presented for the SONLS equation with nonzero boundary conditions. Finally, some conclusions are given in the last section.

## 2. THE IST WITH ZBCs AND BOUND-STATE SOLITON

In this section, we will seek the bound-state soliton  $q(x, t)$  for the SONLS Eq.(1.1) with ZBCs at infinity given by

$$\lim_{x \rightarrow \pm\infty} q(x, t) = 0. \tag{2.1}$$

In what follows, we will present the IST and bound-state soliton for Eq.(1.1) with ZBCs by solving a matrix RHP.

**2.1. The construction of the RHP with ZBCs.** Let  $x \rightarrow \pm\infty$ , the Lax pair (1.3) under the boundary (2.1) can be changed into

$$\phi_x = U_0\phi = ik\sigma_3, \quad \phi_t = V_0\phi = (k + 32\delta k^5)U_0\phi, \tag{2.2}$$

which admits the fundamental matrix solution  $\phi_{bg}(x, t; k)$ , given by

$$\phi^{bg}(x, t; k) = e^{i\Theta(x, t; k)\sigma_3}, \quad \Theta(x, t; k) = k[x + (k + 32\delta k^5)t]. \tag{2.3}$$

Then, we can find the following Jost solutions  $\phi_{\pm}(x, t, ; k)$

$$\phi_{\pm}(x, t; k) \rightarrow e^{i\Theta(x, t; k)\sigma_3}, \quad \text{as } x \rightarrow \pm\infty. \quad (2.4)$$

Further, the modified Jost solutions  $\mu_{\pm}(x, t; k)$  are taken as

$$\mu_{\pm}(x, t; k) = \phi_{\pm}(x, t; k)e^{-i\Theta(x, t; k)\sigma_3}, \quad (2.5)$$

which results in  $\mu_{\pm}(x, t; k) \rightarrow \mathbb{I}$  as  $x \rightarrow \pm\infty$ . Then, the following Volterra integral equations are satisfied

$$\begin{cases} \mu_{-}(x, t; k) = \mathbb{I} + \int_{-\infty}^x \exp[ik\sigma_3(x-y)] Q(y, t)\mu_{-}(y, t; k) \exp[ik\sigma_3(y-x)] dy, \\ \mu_{+}(x, t; k) = \mathbb{I} - \int_x^{+\infty} \exp[ik\sigma_3(x-y)] Q(y, t)\mu_{+}(y, t; k) \exp[ik\sigma_3(y-x)] dy. \end{cases} \quad (2.6)$$

Let  $\mathbb{C}_{\pm} = \{k \in \mathbb{C} | \text{Im}k \gtrless 0\}$  (see Fig. 1). It is not hard to find that the columns  $\mu_{+,1}$  and  $\mu_{-,2}$  are analytic in  $\mathbb{C}_{+}$ , and continuously extended to  $\mathbb{C}_{+} \cup \mathbb{R}$ .  $\mu_{-,1}$  and  $\mu_{+,2}$  are analytic in  $\mathbb{C}_{-}$ , and continuously extended to  $\mathbb{C}_{-} \cup \mathbb{R}$ .

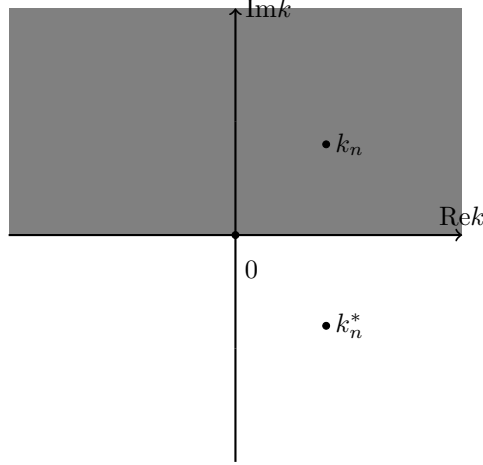


**Figure 1.** (Color online) Distribution of the discrete spectrum and the contours for the RHP on complex  $k$ -plane, Region  $\mathbb{C}_{+}$  (gray region), region  $\mathbb{C}_{-}$  (white region).

In fact, the Jost solutions  $\phi_{\pm}(x, t; k)$  are the simultaneous solutions for the Lax pair (1.3). Therefore,  $\phi_{\pm}(x, t; k)$  have following linear relation by the constant scattering matrix  $S(k) = (s_{ij}(k))_{2 \times 2}$

$$\phi_{+}(x, t; k) = \phi_{-}(x, t; k)S(k), \quad k \in \mathbb{R}, \quad (2.7)$$

or

$$\mu_{+}(x, t; k) = \mu_{-}(x, t; k)e^{i\Theta\sigma_3}S(k)e^{-i\Theta\sigma_3}, \quad k \in \mathbb{R}, \quad (2.8)$$

where  $S(k) = \sigma_2 S^*(k^*) \sigma_2$ ,  $s_{11}(k) = s_{22}^*(k^*)$ ,  $s_{12}(k) = -s_{21}^*(k^*)$ , and  $\sigma_2 = \begin{pmatrix} 0 & -i \\ i & 0 \end{pmatrix}$ . Due to the scattering coefficients can be expressed as the following Wronskians determinant form

$$\begin{aligned} s_{11}(k) &= Wr(\phi_{+,1}, \phi_{-,2}), & s_{12}(k) &= Wr(\phi_{+,2}, \phi_{-,2}), \\ s_{21}(k) &= Wr(\phi_{-,1}, \phi_{+,1}), & s_{22}(k) &= Wr(\phi_{-,1}, \phi_{+,2}), \end{aligned} \quad (2.9)$$

we find that  $s_{11}$  can be analytic continuation to  $\mathbb{C}_{+}$ , and analogously  $s_{22}$  is analytic in  $\mathbb{C}_{-}$ . In addition,  $s_{11}, s_{22} \rightarrow 1$  as  $k \rightarrow \infty$  in  $\mathbb{C}_{+}, \mathbb{C}_{-}$  respectively.

In order to construct a RHP for the inverse spectral problem, we consider the following sectionally meromorphic matrices

$$M_{+}(x, t, k) = \begin{pmatrix} \frac{\mu_{+,1}}{s_{11}} & \\ & \mu_{-,2} \end{pmatrix}, \quad M_{-}(x, t, k) = \begin{pmatrix} \mu_{-,1} & \\ & \frac{\mu_{+,2}}{s_{22}} \end{pmatrix}, \quad (2.10)$$

where superscripts  $\pm$  denote analyticity in  $\mathbb{C}_{+}$  and  $\mathbb{C}_{-}$ , respectively. Naturally, a matrix Riemann-Hilbert problem is presented:

**Riemann-Hilbert Problem 1**  $M(k; x, t)$  solve the following RHP:

$$\begin{cases} M(k; x, t) \text{ is analytic in } \mathbb{C} \setminus \mathbb{R}, \\ M_{+}(k; x, t) = M_{-}(x, t, k)G(x, t, k), & k \in \mathbb{R}, \\ M(k; x, t) \rightarrow \mathbb{I}, & k \rightarrow \infty, \end{cases} \quad (2.11)$$

of which the jump matrix  $G(x, t, k)$  is

$$G(x, t, k) = \begin{pmatrix} 1 + |r(k)|^2 & e^{2i\Theta(x, t, k)r^*(k)} \\ e^{-2i\Theta(x, t, k)r(k)} & 1 \end{pmatrix}, \quad (2.12)$$

where  $r(k) = \frac{s_{21}(k)}{s_{11}(k)}$ .

Recalling the symmetry properties of the Jost eigenfunctions and scattering coefficients, we have  $M_+(k) = \sigma_2 M_-^*(k^*) \sigma_2$ . Taking

$$M(x, t; k) = \mathbb{I} + \frac{1}{k} M^{(1)}(x, t; k) + O\left(\frac{1}{k^2}\right), \quad k \rightarrow \infty, \quad (2.13)$$

then the potential  $q(x, t)$  of the SONLS equation with ZBCs is given by

$$q(x, t) = 2M_{21}^{(1)}(x, t, k) = \lim_{k \rightarrow \infty} 2kM_{21}(x, t, k). \quad (2.14)$$

**2.2. Bound-state soliton with one higher-order pole.** In general, there are exactly discrete spectral points  $k$  in  $\mathbb{C}_+$  which make  $s_{11}(k) = 0$  and those discrete spectral points in  $\mathbb{C}_-$  lead to  $s_{22}(k) = 0$ . Without considering simple poles, we here assume that  $s_{11}(k)$  has  $N$  higher-order poles  $k_n$ ,  $n = 1, 2, \dots, N$ , in  $\mathbb{C}_+$ , that means

$$\begin{aligned} s_{11}(k) &= (k - k_1)^{n_1} (k - k_2)^{n_2} \times \dots \times (k - k_N)^{n_N} s_{11}^{(0)}(k), \\ s_{22}(k) &= (k - k_1^*)^{n_1} (k - k_2^*)^{n_2} \times \dots \times (k - k_N^*)^{n_N} s_{22}^{(0)}(k), \end{aligned} \quad (2.15)$$

where  $s_{11}^{(0)}(k) = s_{22}^{(0)*}(k^*) \neq 0$  for all  $k \in \mathbb{C}_+$ . The symmetric relation of the scattering matrix yields

$$s_{11}(k_n) = s_{22}^*(k_n^*) = 0. \quad (2.16)$$

Thus, the corresponding discrete spectral point set is

$$\Gamma = \{k_n, k_n^*\}_{n=1}^N, \quad (2.17)$$

whose distributions are shown in Fig. 1.

To obtain the explicit soliton solutions, we consider the reflectionless potential of the SONLS equation with ZBCs i.e.,  $r(k) = 0$ . As a matter of convenience, we will show the case of one higher-order pole. This case implies  $s_{11}(k)$  has one  $N$ th order zero point on the upper half plane, i.e.,  $s_{11}(k) = (k - k_0)^N s_{11}^{(0)}(k) (\text{Im} k > 0, N > 1, s_{11}^{(0)}(k_0) \neq 0)$ . As well, we know that  $M_{11}(x, t, k)$  has one  $N$ th order pole at  $k = k_0$ , and  $M_{12}(x, t, k)$  has one  $N$ th order pole at  $k = k_0^*$ . According to normalization condition of matrix  $M(x, t, k)$ , we can write the RHP in the following form

$$M_{11}(x, t, k) = 1 + \sum_{n=1}^N \frac{F_n(x, t)}{(k - k_0)^n}, \quad M_{12}(x, t, k) = \sum_{n=1}^N \frac{G_n(x, t)}{(k - k_0^*)^n}. \quad (2.18)$$

Simultaneously, defining

$$\begin{aligned} e^{-2i\Theta} &= \sum_{s=0}^{+\infty} f_s(x, t) (k - k_0)^s, \quad M_{12}(x, t, k) = \sum_{s=0}^{+\infty} g_s(x, t) (k - k_0)^s, \\ e^{2i\Theta} &= \sum_{s=0}^{+\infty} f_s^*(x, t) (k - k_0^*)^s, \quad M_{11}(x, t, k) = \sum_{s=0}^{+\infty} \varrho_s(x, t) (k - k_0^*)^s, \\ r(k) &= r_0(k) + \sum_{m=1}^N \frac{r_m}{(k - k_0)^m}, \quad r^*(k^*) = r_0^*(k^*) + \sum_{m=1}^N \frac{r_m^*}{(k - k_0^*)^m}, \end{aligned} \quad (2.19)$$

where

$$\begin{aligned} f_s(x, t) &= \lim_{k \rightarrow k_0} \frac{1}{s!} \frac{\partial^s}{\partial k^s} e^{-2i\Theta}, \quad g_s(x, t) = \lim_{k \rightarrow k_0} \frac{1}{s!} \frac{\partial^s}{\partial k^s} M_{12}(x, t, k), \\ \varrho_s(x, t) &= \lim_{k \rightarrow k_0^*} \frac{1}{s!} \frac{\partial^s}{\partial k^s} M_{11}(x, t, k), \quad r_m = \lim_{k \rightarrow k_0} \frac{1}{(N - m)!} \frac{\partial^{N-m}}{\partial k^{N-m}} [(k - k_0)^N r(k)], \\ s &= 0, 1, 2, 3, \dots, m = 1, 2, 3, \dots, N, \end{aligned} \quad (2.20)$$

and  $r_0(k)$  is analytic on the upper half plane.

According to the RHP 1, (2.18), and (2.19), we can collect the associated coefficients of  $(k - k_0)^{-n}$  and  $(k - k_0^*)^{-n}$ , which leads to

$$\begin{aligned} F_n(x, t) &= \sum_{j=n}^N \sum_{s=0}^{j-n} r_j f_{j-n-s}(x, t) g_s(x, t), \\ G_n(x, t) &= - \sum_{j=n}^N \sum_{s=0}^{j-n} r_j^* f_{j-n-s}^*(x, t) \varrho_s(x, t), \quad n = 1, 2, \dots, N. \end{aligned} \quad (2.21)$$

Furthermore, putting (2.18) into  $g_s, \varrho_s$  given in (2.20), we obtain following results

$$\begin{aligned} g_s(x, t) &= \sum_{n=1}^N \binom{n+s-1}{s} \frac{(-1)^s G_n}{(k_0 - k_0^*)^{n+s}}, \quad s = 0, 1, 2, \dots \\ \varrho_s(x, t) &= \begin{cases} 1 + \sum_{n=1}^N \frac{F_n}{(k_0^* - k_0)^n}, & s = 0, \\ \sum_{n=1}^N \binom{n+s-1}{s} \frac{(-1)^s F_n}{(k_0^* - k_0)^{n+s}}, & s = 1, 2, 3, \dots \end{cases} \end{aligned} \quad (2.22)$$

The substitution of (2.22) into (2.21) results in

$$\begin{aligned} F_n(x, t) &= \sum_{j=n}^N \sum_{s=0}^{j-n} \sum_{p=1}^N \binom{p+s-1}{s} \frac{(-1)^s r_j f_{j-n-s}(x, t) G_p}{(k_0 - k_0^*)^{p+s}}, \\ G_n(x, t) &= - \sum_{j=n}^N r_j^* f_{j-n}^*(x, t) \\ &\quad - \sum_{j=n}^N \sum_{s=0}^{j-n} \sum_{p=1}^N \binom{p+s-1}{s} \frac{(-1)^s r_j^* f_{j-n-s}^*(x, t) F_p}{(k_0^* - k_0)^{p+s}}, \quad n = 1, 2, \dots, N. \end{aligned} \quad (2.23)$$

Ultimately, the following theorem can be summarized:

**Theorem 1** *With the ZBCs at infinity given by (2.1), the  $N$ th order bound-state soliton of the SONLS equation is*

$$q = 2 \left[ 1 - \frac{\det(\mathbb{I} + \Omega \Omega^* + |\chi\rangle\langle P_0|)}{\det(\mathbb{I} + \Omega \Omega^*)} \right], \quad (2.24)$$

where  $\langle P_0| = [1, 0, 0, \dots, 0]_{1 \times N}$ , and

$$\begin{aligned} \Omega &= [\Omega_{np}]_{N \times N} = \left[ \sum_{j=n}^N \sum_{s=0}^{j-n} \binom{p+s-1}{s} \frac{(-1)^s r_j f_{j-n-s}}{(k_0 - k_0^*)^{p+s}} \right], \\ |\chi\rangle &= [\chi_1, \chi_2, \chi_3, \dots, \chi_N]^T, \quad \chi_n(x, t) = - \sum_{j=n}^N r_j^* f_{j-n}^*, \quad n, p = 1, 2, 3, \dots, N. \end{aligned} \quad (2.25)$$

**Proof** *Defining  $|F\rangle = [F_1, F_2, \dots, F_N]^T$ ,  $|G\rangle = [G_1, G_2, \dots, G_N]^T$ , we can rewrite the (2.23) as*

$$|F\rangle = \Omega |G\rangle, \quad |G\rangle = |\chi\rangle - \Omega^* |F\rangle. \quad (2.26)$$

Then, we have

$$|F\rangle = \Omega (\mathbb{I} + \Omega^* \Omega)^{-1} |\chi\rangle, \quad |G\rangle = (\mathbb{I} + \Omega^* \Omega)^{-1} |\chi\rangle. \quad (2.27)$$

Substituting (2.27) into (2.18), we obtain

$$\begin{aligned} M_{11} &= \frac{\det(\mathbb{I} + \Omega^* \Omega + |\chi\rangle\langle P(k)|\Omega)}{\det(\mathbb{I} + \Omega^* \Omega)}, \\ M_{12} &= \frac{\det(\mathbb{I} + \Omega^* \Omega + |\chi\rangle\langle P^*(k^*)|)}{\det(\mathbb{I} + \Omega^* \Omega)} - 1, \end{aligned} \quad (2.28)$$

where  $\langle P(k)| = [\frac{1}{k-k_0}, \frac{1}{(k-k_0)^2}, \dots, \frac{1}{(k-k_0)^N}]$ . In terms of the symmetry relation for matrix  $M$  and (2.14), the Theorem 1 can eventually be proved.

Taking  $N = 2$ , then  $k = k_0$  is a second-order zero point of  $s_{11}$ ,  $r(k)$  can be rewritten as

$$r(k) = r_0(k) + \frac{r_1}{k - k_0} + \frac{r_2}{(k - k_0)^2}, \quad (2.29)$$

and elements of matrix  $\Omega$  are

$$\begin{aligned} \Omega_{11} &= \frac{r_1 f_0}{k_0 - k_0^*} + \frac{r_2 f_1}{k_0 - k_0^*} - \frac{r_2 f_0}{(k_0 - k_0^*)^2}, \\ \Omega_{12} &= \frac{r_1 f_0}{(k_0 - k_0^*)^2} + \frac{r_2 f_1}{(k_0 - k_0^*)^2} - \frac{2r_2 f_0}{(k_0 - k_0^*)^3}, \\ \Omega_{21} &= \frac{r_2 f_0}{k_0 - k_0^*}, \quad \Omega_{22} = \frac{r_2 f_0}{(k_0 - k_0^*)^2}, \end{aligned} \quad (2.30)$$

$|\chi\rangle$  is a column vector defined by

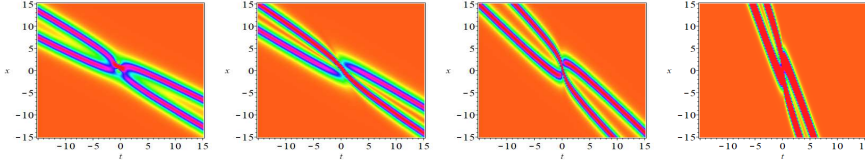
$$\chi_1 = -r_1^* f_0^* - r_2^* f_1^*, \quad \chi_2 = -r_2^* f_0^*, \quad (2.31)$$

and  $\langle P_0 \rangle = [1, 0]$ . For convenience, we have set  $r_1 = r_2 = 1$  and  $k_0 = a + bi$ , in terms of Theorem 1, the second order bound-state soliton solution of the SONLS equation is

$$q(x, t) = \frac{32b^3\Delta_1 e^{-2i\nu_1} + 32b^3\Delta_2 e^{-2i\nu_2}}{(\Delta_3 + 256b^8 e^{4b\nu_3})e^{4b\nu_3}}, \quad (2.32)$$

where

$$\begin{aligned} \nu_1 &= (a + bi)((32b^5\delta i + 160ab^4\delta - 320a^2b^3\delta i - 320a^3b^2\delta \\ &\quad + 160a^4b\delta i + 32a^5\delta + bi + a)t + x), \\ \nu_2 &= (-480a^4b^2\delta + 480a^2b^4\delta - 32b^6\delta + 576a^5b\delta i - 1920a^3b^3\delta i + 576ab^5\delta i \\ &\quad + 32a^6\delta - b^2 + 6abi + a^2)t + (a + 3bi)x, \\ \nu_3 &= (192a^5\delta - 640a^3b^2\delta + 192ab^4\delta + 2a)t + x, \\ \Delta_1 &= (-6144a^5b^5\delta i + 61440a^3b^7\delta i - 30720ab^9\delta i + 30720a^4b^6\delta - 61440a^2b^8\delta \\ &\quad + 6144b^{10}\delta - 64ab^5i + 64b^6)t - 32b^5ix + 16b^5, \\ \Delta_2 &= (384a^5b\delta i - 3840a^3b^3\delta i + 1920ab^5\delta i + 1920a^4b^2\delta - 3840a^2b^4\delta \\ &\quad + 384b^6\delta + 4abi + 4b^2)t + 2bix - 2i + b, \\ \Delta_3 &= (9437184a^{10}b^6\delta^2 + 47185920a^8b^8\delta^2 + 94371840a^6b^{10}\delta^2 + 94371840a^4b^{12}\delta^2 \\ &\quad + 47185920a^2b^{14}\delta^2 + 9437184b^{16}\delta^2 + 196608a^6b^6\delta - 983040a^4b^8\delta - 983040a^2b^{10}\delta \\ &\quad + 196608b^{12}\delta + 1024a^2b^6 + 1024b^8)t^2 + (98304a^5b^6\delta - 983040a^3b^8\delta + 491520ab^{10}\delta \\ &\quad + 1024ab^6)xt + (245760a^4b^7\delta - 491520a^2b^9\delta + 49152b^{11}\delta - 49152a^5b^5\delta + 491520a^3b^7\delta \\ &\quad - 245760ab^9\delta + 512b^7 - 512ab^5)t + 256b^6x^2 + 64b^6 - 256b^5x + 96b^4. \end{aligned} \quad (2.33)$$



(a) (b) (c) (d)

**Figure 2.** (Color online) The density plots of the bound-state soliton solutions (2.32) for Eq.(1.1) with the parameters  $a = \frac{1}{3}, b = \frac{2}{3}$  and (a)  $\delta = 0$ ; (b)  $\delta = \frac{1}{25}$ ; (c)  $\delta = \frac{1}{5}$ ; (d)  $\delta = 1$ .

In fact, the bound-state soliton solutions (2.32) represent the interaction of two-soliton solutions, and the high peak comes from the interaction of two solitons under the degeneration of the associated eigenvalues. The corresponding evolution process of the solutions at different dispersion coefficient  $\delta$  are discussed in Figs. 2. As shown in Fig. 2, we easily find that parameter  $\delta$  affects the phase positions of two solitons.

### 3. THE IST WITH NZBCs AND ROGUE WAVE

In this section, we aim to seek the rogue wave solution  $q(x, t)$  for the SONLS Eq.(1.1) with the following nonzero boundary conditions (NZBCs) as infinity

$$\lim_{x \rightarrow \pm\infty} q(x, t) = Ae^{i(\alpha x + \beta t)}, \quad (3.1)$$

where  $\alpha$  and  $A > 0$  are all real constants,  $\beta = A^2 - \frac{1}{2}\alpha^2 - \delta(\alpha^6 + 90A^4\alpha^2 - 30A^2\alpha^4 - 20A^6)$ .

**3.1. The construction of the RHP with NZBCs.** We devote to derive the RHP of the SONLS equation(1.1) with NZBCs via the robust inverse scattering transform. For any time  $t$ , as  $x \rightarrow \pm\infty$ , the  $q(x, t)$  would tend to a plane wave  $Ae^{i(\alpha x + \beta t)}$ . According to the gauge transformation  $\phi(x, t) = e^{-i(\alpha x + \beta t)\sigma_3/2}\psi(x, t)$ , the Lax pair (1.3) can change into

$$\psi_x = X\psi, \quad \psi_t = T\psi, \quad (3.2)$$

where

$$\begin{aligned} X &= i(k + \frac{\alpha}{2})\sigma_3 + Q_1, \quad Q_1 = \begin{pmatrix} 0 & iq^* e^{i(\alpha x + \beta t)} \\ iq e^{-i(\alpha x + \beta t)} & 0 \end{pmatrix}, \\ T &= e^{i(\alpha x + \beta t)\sigma_3/2} (V + \frac{i\beta\sigma_3}{2}) e^{-i(\alpha x + \beta t)\sigma_3/2}. \end{aligned} \quad (3.3)$$

Let  $x \rightarrow \pm\infty$ , and using the NZBCs(3.1), the following Lax pair will be satisfied

$$\psi_{\pm, x} = X_{\pm}\psi_{\pm}, \quad \psi_{\pm, t} = T_{\pm}\psi_{\pm}, \quad (3.4)$$

where

$$\begin{aligned} X_{\pm} &= i\left(k + \frac{\alpha}{2}\right)\sigma_3 + Q_0, \quad Q_0 = \begin{pmatrix} 0 & iA \\ iA & 0 \end{pmatrix}, \\ T_{\pm} &= \omega(k)X_{\pm} = \left[32\delta k^5 - 16\delta\alpha k^4 - (16\delta A^2 - 8\delta\alpha^2)k^3 + (24\delta\alpha A^2 - 4\delta\alpha^3)k^2 \right. \\ &\quad \left. + (1 - 24\delta\alpha^2 A^2 + 2\delta\alpha^4 + 12\delta A^4)k + 20\delta\alpha^3 A^2 - 30\delta\alpha A^4 - \delta\alpha^5 - \frac{\alpha}{2}\right] X_{\pm}. \end{aligned} \quad (3.5)$$

The fundamental solution of this lax pair is

$$\psi_{\pm}(k; x, t) = n(k) \begin{pmatrix} 1 & \frac{k + \frac{\alpha}{2} - \rho}{A} \\ -\frac{k + \frac{\alpha}{2} - \rho}{A} & 1 \end{pmatrix} e^{i\rho(k)\theta(k; x, t)\sigma_3} = Y(k) e^{i\rho(k)\theta(k; x, t)\sigma_3}, \quad (3.6)$$

where

$$\rho(k)^2 = \left(k + \frac{\alpha}{2}\right)^2 + A^2, \quad n(k)^2 = \frac{\rho + k + \frac{\alpha}{2}}{2\rho}, \quad \theta(k; x, t) = x + \omega(k)t \quad (3.7)$$

The branch cut of  $\rho(k)$  is  $\eta = \eta_+ \cup \eta_-$  with  $\eta_+ = [iA - \frac{\alpha}{2}, -\frac{\alpha}{2}]$  and  $\eta_- = [-iA - \frac{\alpha}{2}, -\frac{\alpha}{2}]$ , of which the branch cut  $\eta$  is oriented upward. (see Fig. 3)

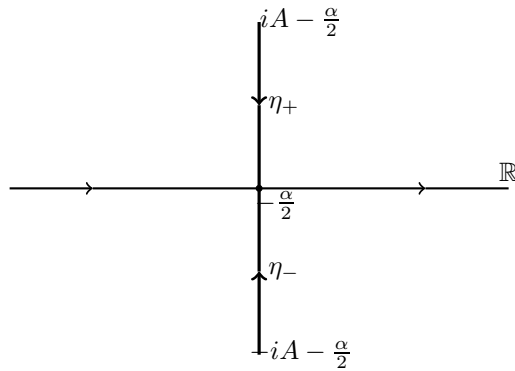


**Figure 3.** (Color online) The contour  $\Sigma_0 = \mathbb{R} \cup \eta$  of the basic RHP.

Then, we assume that  $\Psi_{\pm}(x, t, k)$  also solve the Lax pair in Eq.(3.2), and the asymptotic conditions  $\Psi_{\pm}(x, t, k) \rightarrow \psi_{\pm}(x, t, k)$  as  $x \rightarrow \infty$  should be satisfied. Moreover, taking transformation

$$\mu_{\pm}(x, t, k) = \Psi_{\pm}(x, t, k) e^{-i\rho\theta\sigma_3}, \quad (3.8)$$

we have

$$\mu_{\pm}(x, t, k) \rightarrow Y, \quad x \rightarrow \pm\infty. \quad (3.9)$$

Then it is not hard to calculate the following expression for  $\mu_{\pm}$ , given by

$$\begin{aligned} (Y^{-1}\mu_{\pm})_x + i\rho[Y^{-1}\mu_{\pm}, \sigma_3] &= Y^{-1}(Q_1 - Q_0)\mu_{\pm}, \\ (Y^{-1}\mu_{\pm})_t + i\rho\omega[Y^{-1}\mu_{\pm}, \sigma_3] &= Y^{-1}(T - T_{\pm})\mu_{\pm}, \end{aligned} \quad (3.10)$$

which can be solved by two Volterra integral equations

$$\begin{aligned} \mu_{-}(x, t, k) &= Y + \int_{-\infty}^x Y e^{i\rho(x-y)\hat{\sigma}_3} [Y^{-1}(Q_1 - Q_0)\mu_{-}(y, t, k)] dy, \\ \mu_{+}(x, t, k) &= Y - \int_x^{+\infty} Y e^{i\rho(x-y)\hat{\sigma}_3} [Y^{-1}(Q_1 - Q_0)\mu_{+}(y, t, k)] dy. \end{aligned} \quad (3.11)$$

We first construct the RHP through the robust inverse scattering transform pioneered by Bilman and Miller [36]. At the beginning, we suppose  $q(x, t) - Ae^{\alpha x + \beta t} \in L^1(\mathbb{R})$  and make  $\mu_{\pm} = [\mu_{\pm 1}, \mu_{\pm 2}]$ . Since the first column of  $\mu_{-}$  containing the exponential function  $e^{-2i\rho(x-y)}$ , it can be verified that the first column of  $\mu_{-}$  is analytical on  $\mathbb{C}_{-} \setminus \eta_{-}$ , of which  $\mathbb{C}_{-} = \{k : \text{Im}(\rho) < 0\}$ . Analogously, we find that the second column of  $\mu_{-}$  is analytical on  $\mathbb{C}_{+} \setminus \eta_{+}$ , where  $\mathbb{C}_{+} = \{k : \text{Im}(\rho) > 0\}$ . In conclusion, the  $\mu_{-1}$  and  $\mu_{+2}$  can be analytically continuous to  $\mathbb{C}_{-} \setminus \eta_{-}$ , whereas  $\mu_{-2}$  and  $\mu_{+1}$  can be analytically continuous to  $\mathbb{C}_{+} \setminus \eta_{+}$ .

Due to  $\Psi_{\pm}(x, t, k)$  admit the Lax pair (3.2) for  $k \in \Sigma_0 \setminus \{-\frac{\alpha}{2} \pm iA\}$ , the following scattering relation is presented through scattering matrix  $S(k)$

$$\Psi_{+}(x, t, k) = \Psi_{-}(x, t, k)S(k), \quad k \in \Sigma_0 \setminus \left\{-\frac{\alpha}{2} \pm iA\right\}, \quad (3.12)$$

the scattering matrix  $S(k)$  can be expressed as

$$S(k) = \begin{pmatrix} S_{11}(k) & S_{12}(k) \\ S_{21}(k) & S_{22}(k) \end{pmatrix}, \quad S_{11}(k)S_{22}(k) - S_{12}(k)S_{21}(k) = 1, \quad (3.13)$$

where  $S_{22}(k) = S_{11}(k^*)^*$ ,  $S_{12}(k) = -S_{21}(k^*)^*$ . Then the Beals-Coifman simultaneous solution of (3.2) is

$$\Phi^{BC}(k; x, t) = \begin{cases} \left[ \frac{\Psi_{+1}(k; x, t)}{S_{11}(k)}, \Psi_{-2}(k; x, t) \right], & k \in \mathbb{C}_+ \setminus \eta_+ \\ \left[ \Psi_{-1}(k; x, t), \frac{\Psi_{+2}(k; x, t)}{S_{22}(k)} \right], & k \in \mathbb{C}_- \setminus \eta_- \end{cases} \quad (3.14)$$

Let  $M^{BC}(k; x, t) = \Phi^{BC}(k; x, t)e^{-i\rho\theta\sigma_3}$ , the jumping curve for  $M^{BC}(k; x, t)$  is the  $\mathbb{R} \cup \eta$ . Following the similar computations shown in [46, 47], we can construct another simultaneous solution of the lax pair (3.2) for smaller  $k$  (let's make it  $\epsilon$  here) to make this solution no singularities, given by

$$\Phi(k; x, t) = \begin{cases} \Phi^{BC}(k; x, t), & k \in D_+ \cup D_- \\ \Phi^{in}(k; x, t), & k \in D_0. \end{cases} \quad (3.15)$$

where  $\Phi^{BC}(k; x, t)$  represents the Beals-Coifman simultaneous solution.  $\Phi^{in}(k; x, t)$  is an entire function and can be redefined as  $\Phi(k; x, t)\Phi(k; L, 0)^{-1}$ .  $D_0$  on behalf of the open disk whose boundary is  $\Sigma_+ \cup \Sigma_-$  and radius is  $\epsilon$ . Noteworthily, we should select the appropriate  $\epsilon$  to make the scattering data  $S_{11}(k), S_{22}(k)$  not be zero on the outside of the disk. Simultaneously, the branch cut  $\eta$  should be contained in this disk. As well as, the related domains  $D_{\pm} = \{k \in \mathbb{C} : |k| \geq \epsilon, \text{Im}(k) \gtrless 0\}$  and  $\Sigma = (-\infty, -\epsilon] \cup [\epsilon, +\infty) \cup \Sigma_+ \cup \Sigma_-$  are shown (see Fig. 4). Set  $M(k; x, t) = \Phi(k; x, t)e^{-i\rho\theta\sigma_3}$ , then the RHP of the SONLS equation with NZBCs is:

**Riemann-Hilbert Problem 2**  $M(k; x, t)$  solve the following RH problem:

$$\begin{cases} M(k; x, t) \text{ is analytic in } \mathbb{C} \setminus \{\Sigma \cup \eta\}, \\ M_+(k; x, t) = \begin{cases} M_-(k; x, t)e^{i\rho\theta\sigma_3}J(k; x, t)e^{-i\rho\theta\sigma_3}, & k \in \Sigma, \\ M_-(k; x, t)e^{2i\rho_-\theta\sigma_3}, & k \in \eta, \end{cases} \\ M(k; x, t) \rightarrow \mathbb{I}, & k \rightarrow \infty, \end{cases} \quad (3.16)$$

of which the jump matrix  $J(k; x, t)$  given in what follows,

$$J(k; x, t) = \begin{cases} \left[ \frac{\Psi_{+1}(k; L, 0)}{S_{11}(k)}, \Psi_{-2}(k; L, 0) \right], & k \in \Sigma_+ \\ \left[ \Psi_{-1}(k; L, 0), \frac{\Psi_{+2}(k; L, 0)}{S_{22}(k)} \right]^{-1}, & k \in \Sigma_- \\ \begin{bmatrix} 1 + |R(k)|^2 & R^*(k) \\ R(k) & 1 \end{bmatrix}, & k \in (-\infty, -\epsilon] \cup [\epsilon, +\infty), \end{cases} \quad (3.17)$$

where  $R(k) = \frac{S_{21}(k)}{S_{11}(k)}$  and the contour is shown in Fig. 4. Then one can also recover the solution of the Eq.(1) in the form

$$q(x, t) = 2 \lim_{k \rightarrow \infty} k M_{21}(k; x, t) e^{i(\alpha x + \beta t)}. \quad (3.18)$$

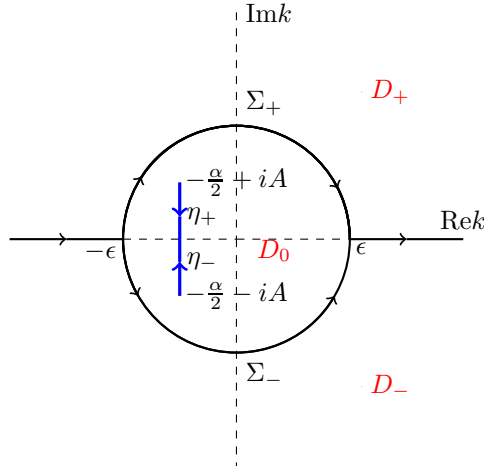


**Figure 4.** (Color online) Definitions of the regions  $D_0, D_{\pm}$  and contours  $\Sigma, \eta$ .

**3.2. Rogue waves of SONLS equation.** In this section, we are aimed at the high-order rogue waves of the SONLS equation by using the modified Darboux transformation for the RHP 2. Take a gauge transformation in what follows

$$\tilde{\Phi}(k; x, t) = \begin{cases} \mathbf{G}(k; x, t)\Phi(k; x, t), & k \in D_+ \cup D_-, \\ \mathbf{G}(k; x, t)\Phi(k; x, t)\mathbf{G}(k; L, 0)^{-1}, & k \in D_0, \end{cases} \quad (3.19)$$

where  $\Phi(k; x, t)$  satisfies the Lax pair (3.2) and yields  $\Phi(k; L, 0) = \mathbb{I}$  for  $k \in D_0$ . The  $\mathbf{G}$  is defined as

$$\mathbf{G}(k; x, t) = \mathbb{I} + \frac{\mathbf{H}(x, t)}{k - \xi} + \frac{\sigma_2 \mathbf{H}^*(x, t) \sigma_2}{k - \xi^*}, \quad (3.20)$$

for any point  $\xi \in D_0$  with  $\mathbf{H}(x, t)$  being written as

$$\mathbf{H}(x, t) = \frac{-(\xi - \xi^*)^2(1 - \vartheta^*(x, t))\mathbf{s}(x, t)\mathbf{s}^T(x, t)\sigma_2 + (\xi - \xi^*)N(x, t)\sigma_2\mathbf{s}^*(x, t)\mathbf{s}^T(x, t)\sigma_2}{-(\xi - \xi^*)^2|1 - \vartheta(x, t)|^2 + N^2(x, t)}, \quad (3.21)$$

of which  $\mathbf{s}(x, t) = \Phi(\xi; x, t)\mathbf{c}$ ,  $N(x, t) = \mathbf{s}^\dagger(x, t)\mathbf{s}(x, t)$ ,  $\vartheta(x, t) = \mathbf{s}^T(x, t)\sigma_2\mathbf{s}'(x, t)$ , and  $\mathbf{c} = (c_1, c_2)^T$  is an arbitrary column vector. Then, the corresponding jump condition of matrix  $\tilde{M}(k; x, t) = \tilde{\Phi}(k; x, t)e^{-i\rho\theta\sigma_3}$  make a difference when  $k \in \Sigma_+ \cup \Sigma_-$ , and the corresponding jump matrix  $J(k)$  is replaced by

$$\tilde{J}(k; x, t) = \begin{cases} \mathbf{G}(k; L, 0)J(k; x, t), & k \in \Sigma_+, \\ J(k; x, t)\mathbf{G}(k; L, 0)^{-1}, & k \in \Sigma_-. \end{cases} \quad (3.22)$$

Similarly, the potential function  $\tilde{q}(x, t)$  can be recovered from the new RHP  $\tilde{M}(k; x, t)$ , that is

$$\tilde{q}(x, t) = 2 \lim_{k \rightarrow \infty} k \tilde{M}_{21}(k; x, t) e^{i(\alpha x + \beta t)} = q(x, t) + 2(\mathbf{H}_{21} - \mathbf{H}_{12}^*) e^{i(\alpha x + \beta t)}. \quad (3.23)$$

In addition, as we make  $\mathbf{c}$  become the form  $\epsilon^{-1}\mathbf{c}_\infty$  with  $\mathbf{c}_\infty \in \mathbb{C}^2 \setminus \{0\}$  being a fixed vector and let  $\epsilon$  tend to 0, then the matrix  $\mathbf{G}(k; x, t)$  can also be taken a limit process, given by

$$\mathbf{G}_\infty(k; x, t) = \mathbb{I} + \frac{\mathbf{H}_\infty(x, t)}{k - \xi} + \frac{\sigma_2 \mathbf{H}_\infty^*(x, t) \sigma_2}{k - \xi^*}, \quad (3.24)$$

where  $\mathbf{H}_\infty(x, t) = \lim_{\epsilon \rightarrow \infty} \mathbf{H}(x, t)$ .

In order to apply the Darboux transformation, the vector  $\mathbf{s}(x, t)$  should be given first. Therefore, in terms of the background eigenvector matrix  $\Phi_{bg}(k; x, t) = \psi_\pm(k; x, t)$ ,  $\Phi_{bg}^{in}(k; x, t) = \Phi_{bg}(k; x, t)\Phi_{bg}(k; 0, 0)^{-1}$  can be regarded as the basic solutions, then one has

$$\Phi_{bg}^{in}(k; x, t) = \frac{\sin(\rho(k)\theta(k; x, t))}{\rho(k)} X_\pm + \cos(\rho(k)\theta(k; x, t)) \mathbb{I}. \quad (3.25)$$

Furthermore, we have

$$\mathbf{s}(\xi; x, t) = \Phi_{bg}^{in}(\xi; x, t)\mathbf{c} = i\gamma(\xi, x, t) \left[ \left( \xi + \frac{\alpha}{2} \right) \sigma_3 \mathbf{c} + A \sigma_1 \mathbf{c} \right] + \chi(\xi, x, t) \mathbf{c}. \quad (3.26)$$

where

$$\sigma_1 = \begin{pmatrix} 0 & 1 \\ 1 & 0 \end{pmatrix}, \quad \gamma(\xi, x, t) = \frac{\sin(\rho(\xi)\theta(\xi; x, t))}{\rho(\xi)}, \quad \chi(\xi, x, t) = \cos(\rho(\xi)\theta(\xi; x, t)) \quad (3.27)$$

and

$$\begin{aligned} N(x, t) &= \mathbf{s}^\dagger(x, t)\mathbf{s}(x, t) = \left[ \left( \xi + \frac{\alpha}{2} \right) \left( \xi^* + \frac{\alpha}{2} \right) |\gamma|^2 + |\chi|^2 + A^2 |\gamma|^2 \right] \mathbf{c}^\dagger \mathbf{c} \\ &+ \left[ i \left( \xi + \frac{\alpha}{2} \right) \gamma \chi^* - i \left( \xi^* + \frac{\alpha}{2} \right) \gamma^* \chi \right] \mathbf{c}^\dagger \sigma_3 \mathbf{c} + [iA\gamma\chi^* - iA\gamma^*\chi] \mathbf{c}^\dagger \sigma_1 \mathbf{c} + i(\xi^* - \xi)A|\gamma|^2 \mathbf{c}^\dagger \sigma_2 \mathbf{c}, \end{aligned} \quad (3.28)$$

$$\begin{aligned} \vartheta(x, t) &= \mathbf{s}^T(x, t)\sigma_2\mathbf{s}'(x, t) = \left[ \gamma\chi' \left( \xi + \frac{\alpha}{2} \right) - \gamma'\chi \left( \xi + \frac{\alpha}{2} \right) - \gamma\chi \right] \mathbf{c}^T \sigma_1 \mathbf{c} \\ &+ \left[ \gamma\gamma' \left( \xi + \frac{\alpha}{2} \right)^2 + \gamma^2 \left( \xi + \frac{\alpha}{2} \right) + \gamma\gamma' A^2 + \chi\chi' \right] \mathbf{c}^T \sigma_2 \mathbf{c} + (A\gamma'\chi - A\gamma\chi') \mathbf{c}^T \sigma_3 \mathbf{c} - iA\gamma^2 \mathbf{c}^T \mathbf{c}, \end{aligned} \quad (3.29)$$

Finally, the solutions of Eq.(1.1) are

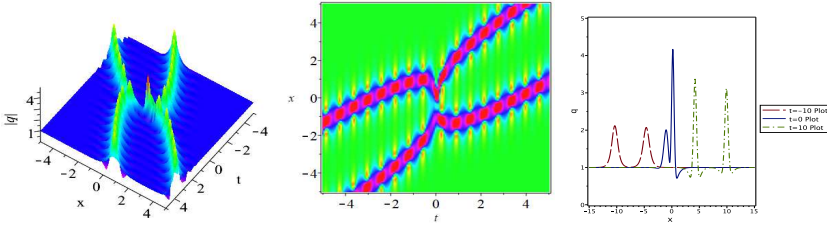
$$\tilde{q}(x, t) = \left( A + \frac{2i(\xi - \xi^*)^2 [(1 - \vartheta^*)s_2^2 - (1 - \vartheta)s_1^{*2}] + 4(\xi - \xi^*)N s_1^* s_2}{(\xi - \xi^*)^2 |1 - \vartheta|^2 - N^2} \right) e^{i(\alpha x + \beta t)}, \quad (3.30)$$

where  $\mathbf{s}$ ,  $N$ ,  $\vartheta$  are given in (3.26), (3.28), (3.29). Moreover, setting  $\mathbf{c} = \mathbf{c}_\infty \epsilon^{-1}$  with  $\epsilon \rightarrow 0$ , the solution (3.30) is changed into

$$\tilde{q}_\infty(x, t) = \left( A - \frac{2i(\xi - \xi^*)^2 (\vartheta_\infty^* s_{\infty 2}^2 - \vartheta_\infty s_{\infty 1}^{*2}) - 4(\xi - \xi^*)N_\infty s_{\infty 1}^* s_{\infty 2}}{(\xi - \xi^*)^2 |\vartheta_\infty|^2 - N_\infty^2} \right) e^{i(\alpha x + \beta t)}, \quad (3.31)$$

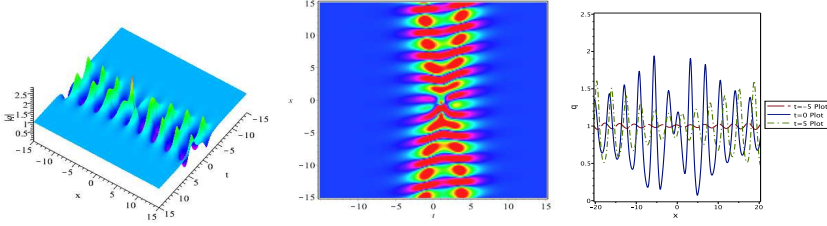
where  $\mathbf{s}_\infty$ ,  $N_\infty$ ,  $\vartheta_\infty$  are given in (3.26), (3.28), (3.29) with  $\mathbf{c}$  substituted by  $\mathbf{c}_\infty$ , respectively.

Based on the theorem spectral analysis, when choosing different  $\xi$ , the corresponding solution properties are very different. For the case of  $\xi = -\frac{\alpha}{2} + i\lambda A$  with  $|\lambda| > 1$ , it becomes the temporal-spatial periodic breather waves, which can be attested by Fig. 5. But when  $|\lambda| < 1$ , as we can see in Fig. 6, it turns into the spatial periodic breather waves.



(a) (b) (c)

**Figure 5.** (Color online) The temporal-spatial periodic breather waves (3.30) for Eq.(1.1) with the parameters  $A = 1, \alpha = \frac{1}{10}, \delta = 0.01, \lambda = \frac{3}{2}, c_1 = i, c_2 = i + 1$ . (a) Three dimensional plot; (b) The density plot; (c) The wave propagation along the  $x$ -axis with  $t = -10$  (long-dashed line),  $t = 0$  (solid line),  $t = 10$  (dash-dotted line).



(a) (b) (c)

**Figure 6.** (Color online) The spatial periodic breather waves (3.30) for Eq.(1.1) with the parameters  $A = 1, \delta = 0.01, \alpha = \frac{1}{10}, \lambda = \frac{1}{2}, c_1 = i, c_2 = i + 1$ . (a) Three dimensional plot; (b) The density plot; (c) The wave propagation along the  $x$ -axis with  $t = -5$  (long-dashed line),  $t = 0$  (solid line),  $t = 5$  (dash-dotted line).

In order to obtain the rogue wave, we should take  $\xi = -\frac{\alpha}{2} \pm iA$  (here  $|\lambda| = \pm 1$ ). For the sake of convenience, we study rogue waves with  $\xi = -\frac{\alpha}{2} + iA$  (it is similar when  $\xi = -\frac{\alpha}{2} - iA$ ). Then, we have

$$\mathbf{s}(x, t) = \begin{pmatrix} i\theta(\xi)A(ic_1 + c_2) + c_1 \\ \theta(\xi)A(ic_1 + c_2) + c_2 \end{pmatrix}, \quad (3.32)$$

$$\mathbf{s}'(x, t) = \begin{pmatrix} \frac{1}{3}A(A\theta^3 + 3i\theta')(ic_1 + c_2) - ic_1\theta(A\theta - 1) \\ -\frac{i}{3}A(A\theta^3 + 3i\theta')(ic_1 + c_2) - ic_2\theta(A\theta + 1) \end{pmatrix}, \quad (3.33)$$

$$N = 2A \left( A\theta(c_1^2 + c_2^2) - \frac{1}{2}(c_1 + ic_2)^2 \right) + A\theta(ic_1 + c_2)^2 + c_1^2 + c_2^2, \quad (3.34)$$

$$\vartheta = -iA\theta^2(c_1^2 + c_2^2) - A\theta'(ic_1 + c_2)^2 + \frac{2}{3}iA^2\theta^3(c_1^2 - c_2^2) + \left(\frac{4}{3}A^2\theta^3 - 2\theta\right)c_1c_2. \quad (3.35)$$

It is not difficult to see that the first-order rogue wave can be derived when  $c_1 = ic_2$ . For instance, let  $c_2 = 1$ , the first-order rogue wave solution is expressed as

$$\tilde{q}(x, t) = \left( \frac{2A \left( (iA^2 - 2A^2\theta - 2A)\theta^* + (2A - iA^2)\theta - 2iA - \frac{A^2}{2} + \frac{3}{2} \right)}{2A^2(i - 2\theta)\theta^* - 2iA^2\theta - A^2 - 1} \right) e^{i(\alpha x + \beta t)}. \quad (3.36)$$

In order to make the rogue wave center being at the origin, we set  $c_\infty = (ic, c)^T$  at (3.31). The exact formula of first-order rogue wave can be shown with  $c = 1$

$$\tilde{q}(x, t) = \left( \frac{A(4A^2\theta\theta^* + 4A\theta^* - 4A\theta - 3)}{4A^2\theta\theta^* + 1} \right) e^{i(\alpha x + \beta t)}, \quad (3.37)$$

whose maximum amplitude is equal to  $3A$ , which is different with the amplitude given in (3.36). Obviously, there are three free parameters  $A, \alpha$  and  $\delta$  in Eq.(3.37). Here, parameter  $A$  determines the amplitude of wave and the height of the background wave. Especially, the effects of  $\alpha$  and  $\delta$  on the dynamic behavior of the rogue wave (3.37) are analyzed respectively in what follows.

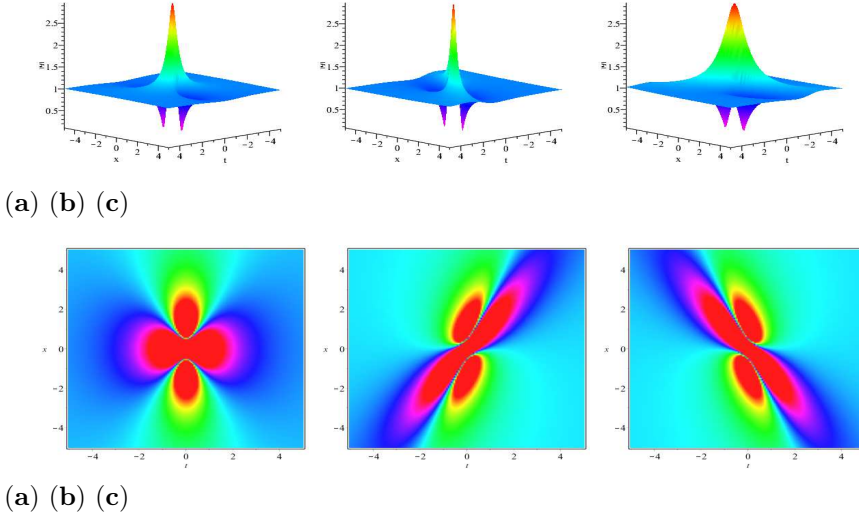


**Figure 7.** (Color online) Three dimensional plots and density plots of the first-order rogue wave (3.37) for Eq.(1.1) with the parameters  $A = 1, \delta = 0.01$ : (a,d)  $\alpha = 0$ , (b,e)  $\alpha = 0.5$ , (c,f)  $\alpha = -0.5$ .

In Fig.7, fixing  $\delta = 0.01$ , we mainly analyse the effect of  $\alpha$  on the wave through different selections of parameter  $\alpha$ . Compared with  $\alpha = 0$ , the ridge direction of the rogue waves turns clockwise for  $\alpha > 0$ , and it turns counter clockwise at the case of  $\alpha < 0$ . As well as, the increase of parameter  $|\alpha|$  leads to the increase of the angle between the ridge of the rogue waves and the  $x$ -axis. As displayed in Fig.8, for fixed parameter  $\alpha = 0$ , we analyse the corresponding evolution process of the rogue wave at different dispersion coefficient  $\delta$ . It is easily to find the fact that the higher order dispersion coefficient  $\delta$  affect the phase of rogue waves. When  $\delta$  increases, the ridge of the rogue wave gradually disappears. On the contrary, the length of the trough becomes more and more larger. Besides, the width of the rogue wave decrease as  $\delta$  increases. It is worth mentioning that the Fig.8 (a)(d) depict the rogue wave for the standard NLS equation with  $\delta = 0$ .

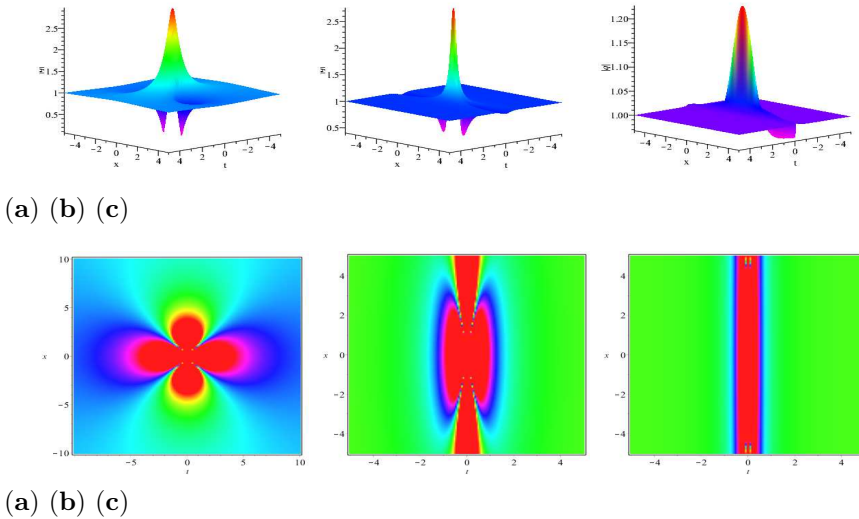


**Figure 8.** (Color online) Three dimensional plots and density plots of the first-order rogue wave (3.37) for Eq.(1.1) with the parameters  $A = 1, \alpha = 0$ : (a,d)  $\delta = 0$ , (b,e)  $\delta = 0.1$ , (c,f)  $\delta = 1$ .

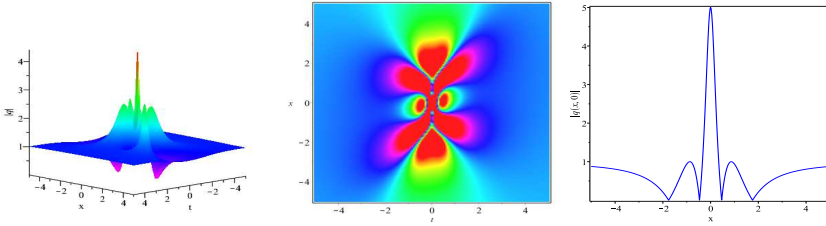
On the other hand, taking  $c_\infty = (1, i)^T$  in (3.31), we will have the second-order rogue wave

$$\tilde{q}(x, t) = \frac{\tilde{\omega}_2}{\tilde{\omega}_1} e^{i(\alpha x + \beta t)}, \quad (3.38)$$

where

$$\begin{aligned}
\Xi_1 &= -64A^6\theta^*3\theta^3 + 96iA^5\theta^*3\theta' + 48A^4\theta^*3\theta - 144A^4\theta^*2\theta^2 + 48A^4\theta^*\theta^3 \\
&\quad - 72iA^3\theta^*\theta' - 108A^2\theta^*\theta - 96iA^5\theta^*\theta^3 + 72iA^3\theta^*\theta - 144A^4\theta^*\theta' - 9, \\
\Xi_2 &= -64A^7\theta^*3\theta^3 - 288iA^5\theta^*2\theta' - 192A^6\theta^*3\theta^2 - 144A^5\theta^*3\theta - 48A^4\theta^*3 \\
&\quad + 192A^6\theta^*2\theta^3 - 216iA^4\theta^*\theta + 432A^5\theta^*2\theta^2 + 144A^4\theta^*2\theta - 144A^5\theta^*\theta^3 \\
&\quad - 72iA^3\theta' - 144A^4\theta^*\theta^2 + 180A^3\theta^*\theta + 108A^2\theta^* - 288iA^5\theta^*\theta^2 - 72iA^3\theta^* \\
&\quad - 96iA^6\theta^*\theta^3 - 144A^5\theta^*\theta' + 96iA^6\theta^*3\theta' + 48A^4\theta^3 \\
&\quad + 216iA^4\theta^*\theta' - 108A^2\theta - 45A,
\end{aligned} \tag{3.39}$$

and the dynamic behavior of the second-order rogue wave is shown in the following pictures.



(a) (b) (c)

**Figure 9.** (Color online) The second-order rogue wave (3.38) for Eq.(1.1) with the parameters  $A = 1, \delta = 0.01, \alpha = \frac{1}{10}$ . (a) Three dimensional plot; (b) The density plot; (c) The wave propagation along the  $x$ -axis at  $t = 0$ .

#### 4. CONCLUSION

In this paper, we first researched the bound-state soliton with one higher-order pole for the SONLS equation at ZNCs via using Laurent's series and generalization of the residue theorem. Then, we discussed the corresponding dynamic behavior of the solutions, and indicated that the parameter  $\delta$  could decide the waveform and distance between two waves. We also have used the robust inverse scattering transform to derived the breather wave and rogue wave solutions for the SONLS equation with arbitrary NZBCs. Based on the one-fold DT, we obtained the first order rogue wave solution for  $c = (ic, c)^T$  and second rogue wave solution for  $c_\infty = (1, i)^T$ . Besides, we found that the amplitude of rogue wave only depends on boundary conditions  $A$ . Furthermore, we also analysed the effect of parameter  $\alpha$  and the higher order terms  $\delta$  on the wave through choosing different parameter  $\alpha$  and  $\delta$ . The technique shown in this paper can be generalized to some other nonlinear systems and more meaningful phenomena will be presented by certain further research.

#### REFERENCES

- [1] Matveev V B, Salle M A 1991 Darboux Transformation and Solitons. Berlin: Springer.
- [2] Hirota R 2004 Direct Methods in Soliton Theory. Berlin: Springer.
- [3] Ablowitz M J, Clarkson P A 1991 Solitons; Nonlinear Evolution Equations and Inverse Scattering. Cambridge: Cambridge University Press.
- [4] Bluman G W, Kumei S 1989 Symmetries and Differential Equations, Springer-Verlag, New York.
- [5] Gardner C S, Greene J M, Kruskal M D, Miura R M 1967 Method for solving the Korteweg-de Vries equation. Phys. Rev. Lett. 19 1095.
- [6] Zakharov V E, Manakov S V, Novikov S P, Pitaevskii L P 1984 The Theory of Solitons: The Inverse Scattering Method, New York: Consultants Bureau.
- [7] Ma W X 2018 Riemann-Hilbert problems and  $N$ -soliton solutions for a coupled mKdV system. J. Geom. Phys. 132 45-54.
- [8] Guo B L, Ling L M 2012 Riemann-Hilbert approach and  $N$ -soliton formula for coupled derivative Schrödinger equation. J. Math. Phys. 53 133-3966.
- [9] Liu N, Guo B L 2021 Painlevé-type asymptotics of an extended modified KdV equation in transition regions. J. Differ. Equations, 280 203-235.
- [10] Geng X G, Wang K D, Chen M M 2021 Long-Time Asymptotics for the Spin-1 Gross-Pitaevskii Equation. Commun. Math. Phys. 1-27.
- [11] Xu J, Fan E G 2015 Long-time asymptotics for the Fokas-Lenells equation with decaying initial value problem: without solitons, J. Differ. Equations, 259 1098-1148.
- [12] Wang D S, Guo B L, Wang X L 2019 Long-time asymptotics of the focusing Kundu-Eckhaus equation with nonzero boundary conditions. J. Diff. Equations, 266(9) 5209-5253.
- [13] Yang J 2010 Nonlinear Waves in Integrable and Non-integrable Systems. Society for Industrial and Applied Mathematics.
- [14] Jenkins R, McLaughlin K D 2014 The semiclassical limit of focusing NLS for a family of square barrier initial data. Comm. Pure Appl. Math. 67 246-287.
- [15] Deift P, Zhou X 1993 A steepest descent method for oscillatory Riemann-Hilbert problems. Asymptotics for the MKdV equation, Ann. of Math. 137 295-368.
- [16] Biondini G, Mantzavinos D 2017 Long-time asymptotics for the focusing nonlinear Schrödinger equation with nonzero boundary conditions at infinity and asymptotic stage of modulational instability. Comm. Pure Appl. Math. LXX 2300-2365.

- [17] Tian S F 2017 Initial-boundary value problems for the general coupled nonlinear Schrödinger equation on the interval via the Fokas method. *J. Differ. Equations* 262(1) 506-558.
- [18] Zakharov V E, Shabat A 1972 Exact theory of two-dimensional self-focusing and one dimensional self-modulation of waves in nonlinear media, *Sov. Phys. JETP*, 34(1) 62-69.
- [19] Poppe C 1983 Construction of solutions of the sine-Gordon equation by means of Fredholm determinants, *Physica D*, 9 103-139.
- [20] Tsuru H, Wadati M 1984 The multiple pole solutions of the sine-Gordon equation, *J. Phys. Soc. Japan*, 9 2908-2921.
- [21] Wadati M, Ohkuma K 1981 Multiple pole solutions of the modified Korteweg-de Vries equation, *J. Phys. Soc. Japan*, 51(6) 2029-2035.
- [22] Zhang Y S, Tao X X, Xu S W 2020 The bound-state soliton solutions of the complex modified KdV equation. *Inverse Problems*. 36 065003 (17pp)
- [23] Zhang Y S, Rao J G, Cheng Y, He J S 2019 Riemann-Hilbert method for the Wadati-Konno-Ichikawa equation:  $N$  simple poles and one higher-order pole. *Physica D* 399 173-185.
- [24] Zhang Y S, Tao X X, Yao T T, He J S 2020 The regularity of the multiple higher-order poles solitons of the NLS equation. *Stud. Appl. Math.* 145(4) 812-827.
- [25] Ling L M 2016 The algebraic representation for high order solution of Sasa-Satsuma equation. *Discrete Continuous Dynamical Systems-S*. 9 6.
- [26] Yang B, Chen Y 2019 High-order soliton matrices for Sasa-Satsuma equation via local Riemann-Hilbert problem. *Nonlinear Analysis: Real World Applications* 45 918-941
- [27] Bilman D, Buckingham R 2019 Large-order asymptotics for multiple-pole solitons of the focusing nonlinear Schrödinger equation. *J. Nonlinear Sci.* 29 2185-229.
- [28] Zhang X E, Ling L M 2020 Asymptotic analysis of high order solitons for the Hirota equation. arXiv preprint arXiv:2008.12631.
- [29] Peregrine D H 1983 Water waves, nonlinear Schrödinger equations and their solutions. *J. Aust. Math. Soc. Ser. B: Appl. Math.* 25 16.
- [30] Ma W X, You Y C 2005 Solving the Korteweg-de Vries equation by its bilinear form: Wronskian solutions. *Am. Math. Soc.* 357 1753.
- [31] Wang X B, Tian S F, Zhang T T 2018 Characteristics of the breather and rogue waves in a  $(2+1)$ -dimensional nonlinear Schrödinger equation. *Proc. Am. Math. Soc.* 146 3353.
- [32] Zhang G Q, Yan Z Y, Wen X Y 2018 Modulational instability, beak-shaped rogue waves, multi-dark-dark solitons and dynamics in pair-transition-coupled nonlinear Schrödinger equations. *Proc. R. Soc. A* 473 20170243.
- [33] Peng W Q, Tian S F, Zhang T T 2018 Dynamics of breather waves and higher-order rogue waves in a coupled nonlinear Schrödinger equation. *EPL* 123 50005.
- [34] Wang X, Li Y, Chen Y 2014 Generalized Darboux transformation and localized waves in coupled Hirota equations. *Wave Motion* 51 1149.
- [35] Zhang X E, Chen Y 2018 General high-order rogue waves to nonlinear Schrödinger-Boussinesq equation with the dynamical analysis. *Nonlinear Dyn.* 93 2169-2184.
- [36] Bilman D, Miller P 2019 A robust inverse scattering transform for the focusing nonlinear Schrödinger equation. *Comm. Pure. Appl. Math.* LXXII 1722-1805.
- [37] Chen S Y, Yan Z Y 2019 The Hirota equation: Darboux transform of the Riemann-Hilbert problem and higher-order rogue waves. *Appl. Math. Lett.* 95 65-71.
- [38] Chen S Y, Yan Z Y 2019 The higher-order nonlinear Schrödinger equation with non-zero boundary conditions: robust inverse scattering transform, breathers, and rogons. *Phys. Lett. A* 383 125906.
- [39] Zhang X E, Chen Y 2019 Inverse scattering transformation for generalized nonlinear Schrödinger equation. *Appl. Math. Lett.* 98 306-313.
- [40] Liu N, Guo B L. 2020 Solitons and rogue waves of the quartic nonlinear Schrödinger equation by Riemann-Hilbert approach. *Nonlinear Dyn.* 100 629-646.
- [41] Kedziora D J, Ankiewicz A, Chowdury A, Akhmediev N 2015 Integrable equations of the infinite nonlinear Schrödinger equation hierarchy with time variable coefficients, *Chaos*, 25 103114.
- [42] Su J J, Gao Y T 2017 Bilinear forms and solitons for a generalized sixth-order nonlinear Schrödinger equation in an optical fiber. *Eur Phys J Plus* 132 53.
- [43] Lan Z Z, Guo B L 2018 Conservation laws, modulation instability and solitons interactions for a nonlinear Schrödinger equation with the sextic operators in an optical fiber. *Opt Quantum Electron* 50 340.
- [44] Sun W R 2017 Breather to soliton transitions and nonlinear wave interactions for the nonlinear Schrödinger equation with the sextic operators in optical fibers. *Ann Phys* 529 1600227.
- [45] Yue Y F, Huang L L, Chen Y 2020 Modulation instability, rogue waves and spectral analysis for the sixth-order nonlinear Schrödinger equation *Commun Nonlinear Sci Numer Simulat* 89 105284.
- [46] Defit P, Zhou X 1991 Direct and inverse scattering on the line with arbitrary singularities. *Comm. Pure Appl. Math.* 44 485-533.
- [47] Zhou X 1989 Direct and inverse scattering transformations with arbitrary spectral singularities. *Comm. Pure Appl. Math.* 42 895-938.

(WP) SCHOOL OF MATHEMATICAL SCIENCES, SHANGHAI KEY LABORATORY OF PURE MATHEMATICS AND MATHEMATICAL PRACTICE, EAST CHINA NORMAL UNIVERSITY, SHANGHAI 200062, PEOPLE'S REPUBLIC OF CHINA

(YC) SCHOOL OF MATHEMATICAL SCIENCES, SHANGHAI KEY LABORATORY OF PURE MATHEMATICS AND MATHEMATICAL PRACTICE, EAST CHINA NORMAL UNIVERSITY, SHANGHAI 200062, PEOPLE'S REPUBLIC OF CHINA

(YC) COLLEGE OF MATHEMATICS AND SYSTEMS SCIENCE, SHANDONG UNIVERSITY OF SCIENCE AND TECHNOLOGY, QINGDAO 266590, PEOPLE'S REPUBLIC OF CHINA

(YC) DEPARTMENT OF PHYSICS, ZHEJIANG NORMAL UNIVERSITY, JINHUA 321004, PEOPLE'S REPUBLIC OF CHINA  
*Email address: ychen@sei.ecnu.edu.cn*